Nanodiamond gels in nonpolar media: Colloidal and rheological properties

Nancy A. Burns, Michael A. Naclerio, and Saad A. Khan[a)]

Department of Chemical and Biomolecular Engineering, North Carolina State University, Raleigh, North Carolina 27695-7905

Akbar Shojaei

Department of Chemical and Petroleum Engineering, Sharif University of Technology, Tehran, Iran

Srinivasa R. Raghavan

Department of Chemical and Biomolecular Engineering, University of Maryland, College Park, Maryland 20742-2111

(Received 5 May 2014; final revision received 21 July 2014; published 27 August 2014)

Synopsis

Nanodiamonds (ND), i.e., sp^3-hybridized nanoscale carbon particles, are being widely explored for biomedical applications, such as drug delivery and medical imaging, because of their biocompatibility, nontoxic nature, and ease of surface functionalization. However, little is known about the colloidal and rheological properties of ND dispersions. Here, we report a systematic study on NDs dispersed in a nonpolar liquid, mineral oil. We find that our smallest entities in dispersion are tightly bound aggregates (~400 nm) of individual primary (~5 nm) particles. These aggregates form colloidal gels (with frequency-independent moduli) at low particle concentrations (~5 wt. %). Gelation is likely due to attractive interparticle forces composed of both van der Waals and hydrogen-bonding interactions. The elastic modulus (G'), yield stress (σ_y), and yield strain (γ_0) of these colloidal gels all show scaling relationships with ND concentration, with G' and σ_y exhibiting positive power-law exponents and γ_0 showing a negative one. These results suggest a sample-spanning network of interconnected flocs, each of which is composed of several ND aggregates. Functionalization of ND surfaces with methacrylate groups eliminates gelation and gives a stable, low-viscosity dispersion. Much like other particulate gels, ND gels show thixotropic behavior, i.e., the gel network is disrupted by large deformations (steady or oscillatory shear) and is reformed upon cessation of shear. However, after oscillatory shear at a large strain-amplitude (1000%), the recovery is incomplete and the modulus of the recovered gel is only half its original value. In contrast, near-complete recovery of the modulus is observed after steady shear. © *2014 The Society of Rheology*. [http://dx.doi.org/10.1122/1.4892901]

I. INTRODUCTION

Carbon-based nanomaterials have long received attention due to their chemical stability, thermal conductivity, optical transparency, and other attractive properties which

[a)]Author to whom correspondence should be addressed; electronic mail: khan@eos.ncsu.edu

make them ideal for polymer composites (i.e., highly wear resistant or thermally conductive coatings), optics, biotechnology, and electronic applications. Examples of well-known carbon nanomaterials include carbon nanotubes, fullerenes, graphene, carbon nanofibers, and carbon black [Marchesan *et al*. (2014); Zhang *et al*. (2013)]. A different type of carbon-based nanomaterial that is rapidly gaining worldwide attention is nanodiamonds (NDs). NDs are favored in many applications, especially biomedical ones for their highly tunable surface, biocompatibility, and low toxicity [Schrand *et al*. (2009); Krueger (2008)].

NDs are thermally and chemically stable nanocarbon particles with a diamond core. They are synthesized either via a shock-wave transformation of graphite or the detonation of trinitrotoluene (TNT) and hexogen in an oxygen-poor atmosphere. The resulting spherical particles have a narrow size distribution around 5 nm with a sp^3 core that is covered with multiple surface groups including carboxylic acids, esters, ethers, and lactones (Fig. 1) [Kruger (2008)]. These groups can be removed via thermal or acid treatments; however, spontaneous agglomeration due to particle-particle interactions is prevalent which results in aggregates (~200–400 nm) instead of individual nanoparticles [Lui *et al*. (2012); Xu and Zhao (2012)]. A number of studies have been conducted to examine the disaggregation of NDs aggregates, as they can withstand typical mixing methods. Approaches in this regard include chemical surface modifications, such as fluorination [Liu *et al*. (2004)] or hydroxylation [Krueger (2008)], and robust mechanical methods, that include attrition milling [Krueger *et al*. (2005)] and bead assisted ultra-sonication [Ozawa *et al*. (2007)]. However, commercial NDs typically exist in the aggregate form.

NDs retain all the desirable properties of bulk diamond (i.e., strength, hardness, thermal conductivity, electrical resistivity, optical transparency, etc.) even after surface functionalization, because of their diamond core. These, together with their nanoscale size, make them attractive for a wide range of applications [Mochalin *et al*. (2012); Krueger (2011)]. They are considered to be a nontoxic alternative to quantum dots for use in biomedical imaging and florescence microscopy owing to their high refractive indices and multicolor centers [Hui *et al*. (2010)]. NDs also possess several therapeutic benefits that make them useful for biotechnology applications from labeling and drug delivery to

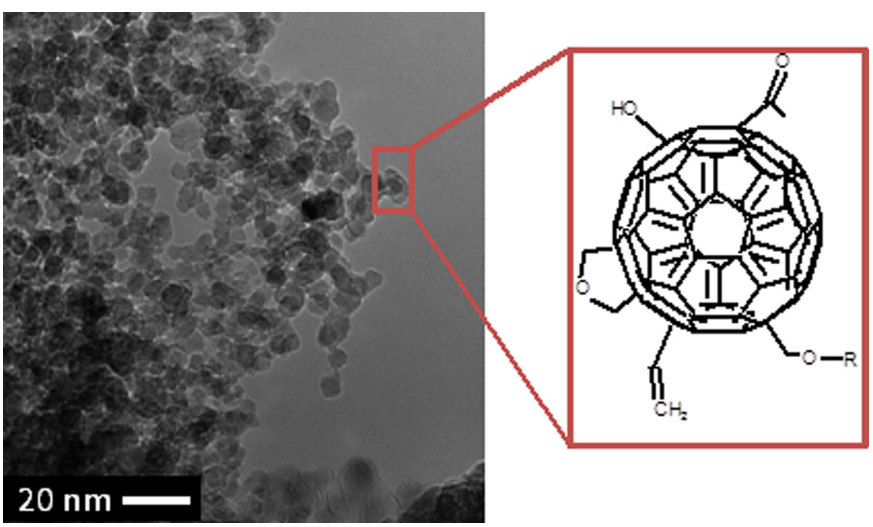

FIG. 1. Transmission electron microscopy image and schematic of NDs [adapted from NanoBlox, DelRay Beach, FL].

tissue engineering and protein separations. For example, research by Thalhammer *et al.* (2010) highlights the use of NDs in regenerative medicine as they have been found to promote neuronal growth similar to protein-coated materials. NDs have also been considered by Kotov (2010) for the transport of genetic materials across cellular membranes, such as the blood–brain barrier, because they can be used to potentially mimic globular proteins. A more extensive list of biomedical applications and therapeutic benefits of NDs can be found in a review by Schrand *et al.* (2009) and Krueger (2008).

Despite the promise of NDs, the rheological behavior of dispersions of these particles remains unexplored. For processing and new materials development, it is necessary to understand and control the rheological properties of ND dispersions. The interactions and modifications that result in a stable ND dispersion or the formation of a flocculated network need to be characterized. In this study, we examine colloidal gels of NDs formed in a nonpolar medium, mineral oil. Mineral oil is used as a model solvent because its nonpolar nature ensures that there are minimal interactions between the nanoparticles and the solvent. Critical issues we seek to understand include the interactions responsible for colloidal gel formation, the effect of nanoparticle content on the modulus of the gel, the effect of large deformations on gel breakdown and structural recovery, and how functionalization of the nanoparticle surface influences rheology. Our study serves as a first step toward understanding the rheology of this unique class of materials.

II. MATERIALS AND METHODS

A. Materials

Light mineral oil, diisobutyl-aluminum hydride (20 wt. % solution in toluene), [3–(methacryloxy) propyl] trimethoxysilane (3-MPTS, 98%), acetone, sodium bicarbonate (>99.7%), sodium hydroxide, and hydrochloride were all purchased from Sigma Aldrich (St. Louis, MO) and used as received. Toluene and ethyl alcohol were purchased from Fisher Scientific (Hampton, NH) and used as received. Purified NDs (75–98 wt. % sp^3 content) were purchased from NanoBlox, Inc. (Delray Beach, FL).

B. Sample preparation

Dispersions of ground ND in mineral oil were prepared by intense mixing for 30 min at 6000 rpm via a Silverson (SL2T) shear mixer to ensure sample homogeneity. The resulting systems were placed under vacuum (10 in Hg) overnight to remove any entrained air bubbles. Care was taken to ensure sample reproducibility which was confirmed via duplicated frequency sweeps. All samples were prepared from as-purchased NDs unless otherwise stated.

C. Rheology

Dynamic rheological experiments were conducted at room temperature (25 °C) on a Rheometric Scientific ARES strain controlled rheometer. Steady state rheological experiments were conducted on a TA Instruments AR2000 stress controlled rheometer. Medium grit Klingspor (PS33, P60) sandpaper covered parallel-plate (25 mm) geometries with a 0.5 mm gap was used to eliminate slip on both rheometers. The use of sandpaper, in lieu of serrated plates, has proven successful in measuring properties of other complex systems [Khan *et al.* (1988)]. The same sample preparation, as explained previously, was used in all cases to ensure reproducibility. The rheological data have been reproduced in triplicate with a relative error of less than ±5%. Measurement of exponents for yield stress and strain had an error of ±10%.

D. Dynamic light scattering

The average hydrodynamic diameter of a very dilute (0.001 wt. %) ND dispersion in mineral oil was determined via dynamic light scattering (DLS) on a Malvern Nano ZS instrument using a 5 mW laser at $\lambda = 633$ nm. A polydispersity index of 0.371 was obtained, and measurements were reproduced six times.

E. ND functionalization

The original ND surfaces were altered using a combination of oxidation, reduction, and functionalization steps. Fourier transform infrared spectroscopy (FTIR) studies were performed after each step to verify conversion. FTIR spectra were obtained using a Nicolet 6700 spectroscope (Thermo Electron Corp) with 256 scans, a resolution of 4 cm^{-1}, and a spectral range of 4000–1000 cm^{-1}.

The oxidation of carbon-based materials removes organic impurities by creating carboxylic acid moieties on the surface. For this purpose, NDs were vacuumed dried (2 h at 80 °C), then heated in a tube furnace for 1.5 h at 425 °C. Then additional impurities were removed via a 24 h HCl reflux, followed by water rinses to neutralize the *p*H. FTIR spectrum shifts and powder color change (dark gray to light brown) were observed, indicating that the oxidation purification step was successful. The carboxylic acid conversion due to oxidation was calculated using Goertzen's (2010) Boehm titration method.

The reduction of the carboxylic acid groups to alcohols was based on procedures by Vast *et al*. (2007) and Irani *et al*. (2013). Briefly, oxidized NDs dispersed in toluene were reacted with an excess of diisobutylaluminum hydride (DIBAL-H) in a nitrogen environment at 0 °C. The amount of DIBAL-H used (4:1 DIBAL-H/carboxylic group) was calculated from the number of carboxylic acid groups determined by the Boehm titration. After completion of the reaction, the product was purified via centrifugation, repeated washes with toluene and ethanol, and vacuum drying.

The reduced NDs were functionalized with 3-MPTS as described by Bag *et al*. (2004). Briefly, reduced NDs (2.5 g) dispersed in toluene (100 ml) were refluxed with an excess of 3-MPTS (20 ml) for 6 h at 100 °C. The product was purified via centrifugation, five repeat washings with water then acetone, and vacuum drying.

III. RESULTS AND DISCUSSION

A. ND gel rheology

We begin by examining very dilute dispersions of NDs in mineral oil via DLS. The average hydrodynamic diameter over six measurements was found to be 388 ± 34.6 nm. This is consistent with previously reported sizes of tightly bound ND aggregates that are resistant to breakdown from high shear mixing or ultra-sonication [Liu *et al*. (2012)]. The existence of aggregates, not single ND particles, is also supported by confocal microscopic images (data not shown) which indicate well distributed aggregates ($\sim$400 nm) throughout the dispersion. The smallest entity or primary unit in our study therefore consists of ND aggregates, hence forth referred to as NDs. Increasing the concentration of these NDs in mineral oil results in a macroscopically homogenous and self-supporting sample, a representative image of which is shown in Fig. 2(a) (inset) Frequency spectra of these NDs (5 and 10 wt. %) in mineral oil show gel-like characteristics [Fig. 2(a)], i.e., a predominant elastic response with the elastic moduli (G') larger than the viscous moduli (G'') and both moduli independent of frequency. Experiments conducted at other ND concentrations showed similar frequency response and even at lower frequencies (e.g.,

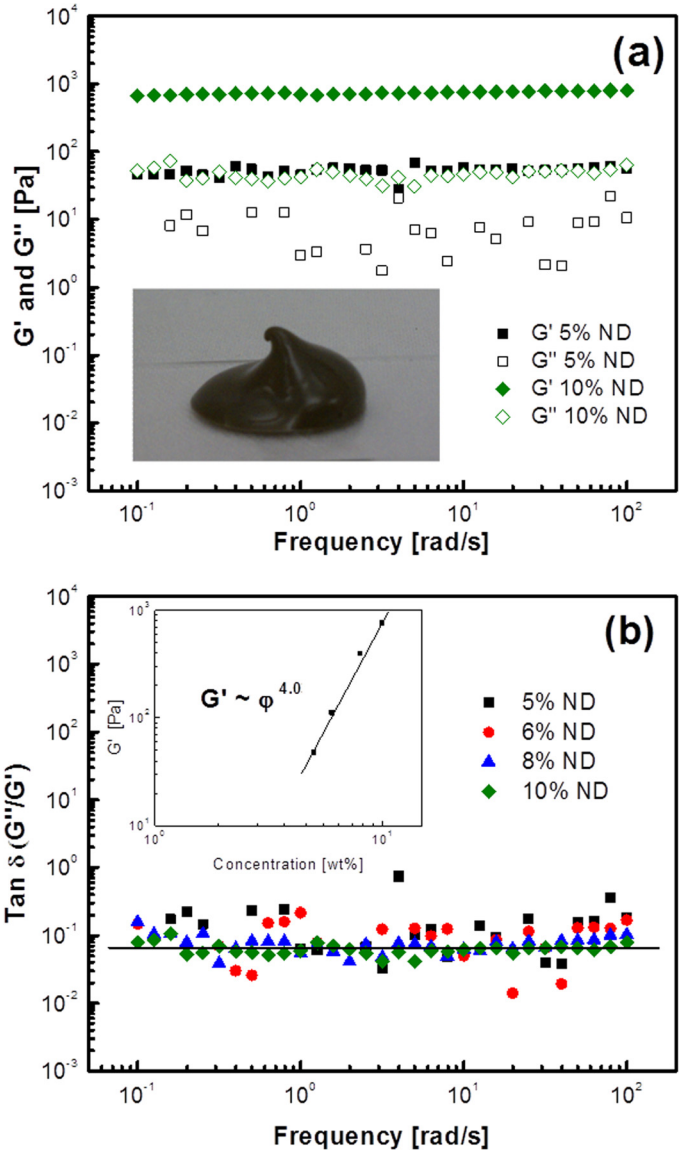

FIG. 2. NDs in mineral oil. (a) Elastic (G′, solid symbols) and viscous (G″, open symbols) moduli of 5 and 10 wt. % NDs are shown as a function of frequency with an embedded image of 10 wt. % NDs supporting their own weight; and (b) tan δ (G″/G′) as a function of frequency for multiple concentrations of NDs. The inset shows a power-law dependence of G′ with filler volume fraction.

0.01 rad/s). A plot of G′ of the gels as a function of ND content (φ) reveals a power-law relationship, i.e., $G' \sim \varphi^4$ [Fig. 2(b) inset]. Such scaling behavior with an exponent approximating 4 is reminiscent of several different attractive or gelling systems including: silica, boehmite alumina, clay, latex, fat, whey proteins, and polystyrene [Khan and Zoeller (1993); Shih *et al*. (1999); Cassagnau (2008); Vreeker *et al*. (1992a, 1992b); Buscall *et al*. (1987); Buscall *et al*. (1988); Shay *et al*. (2001)]. Interestingly, even though the G′ increases substantially with increasing ND content, the loss tangent [Fig. 2(b)] effectively remains constant in this concentration regime. This suggests that while the

number density of interaggregate bonds reflected by G′ increases with ND content, there is an equivalent increase in the viscous nature of the sample.

Figure 3(a) shows the nonlinear oscillatory response of ND gels at various concentrations obtained by conducting strain sweeps from 0.1 to 1000% at a frequency of 1 rad/s. For all concentrations, G′ starts out higher than G″ and then decreases rapidly following structural breakdown, with G″ ultimately dominating. We also observe a maximum in G″ related to breakdown strain [Koumakis and Petekidis (2011)] that shifts to lower values with increasing ND concentration. To ascertain the breakdown more precisely, we have replotted the data in Fig. 3(b) in terms of the elastic stress (product of G′ and strain) as a function of strain [Walls *et al*. (2003)]. The strains corresponding to the maxima in elastic

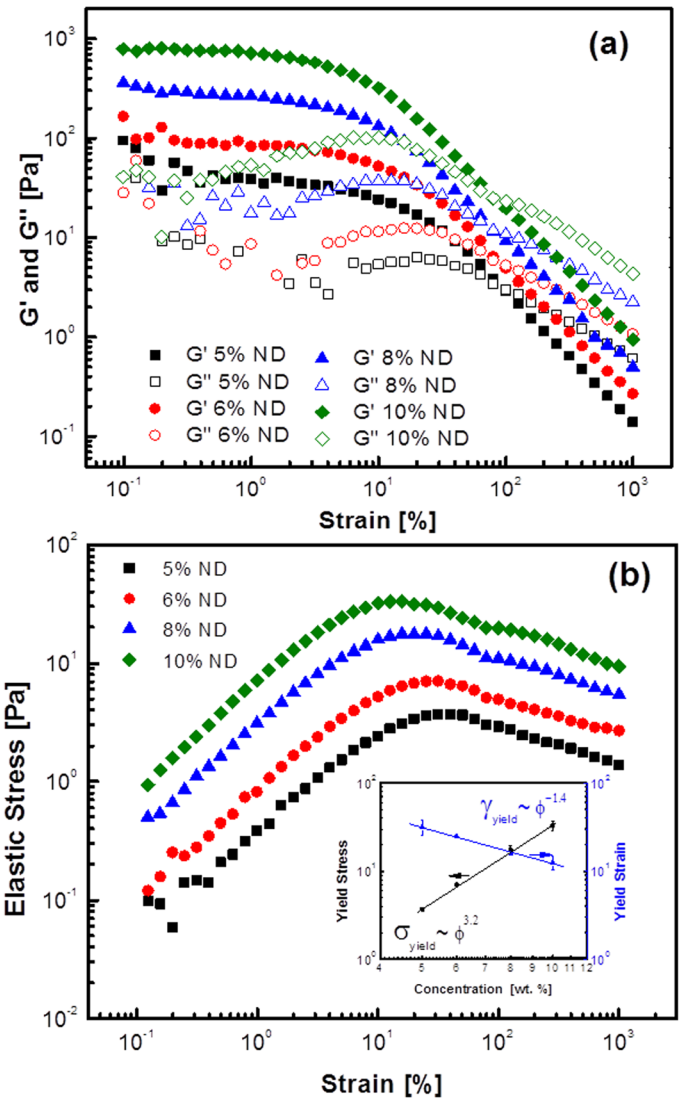

FIG. 3. Dynamic rheology data of NDs at various concentrations in mineral oil (a) with the elastic (G′, solid symbols) and viscous (G″, open symbols) plotted as a function of strain and (b) the elastic stress (G′ γ) plotted as a function of strain percent (γ%). The maxima correspond to the yield point. The yield stress (black squares) and strain (blue triangles) obtained from the maxima are shown as a function of ND concentrations as an inset.

stress represent the yield or breaking strain (γ_0) which follows a power-law behavior with an exponent of approximately -1.3 [Fig. 3(b) inset].

Figure 3(b) also serves to highlight the yield stress of ND gels. While several methods exist to measure yield stress [Moller *et al.* (2006); Walls *et al.* (2003)], the use of elastic stress from dynamic experiments has been found to work well for colloidal systems [Yang *et al.* (1986); Walls *et al.* (2003); Koumakis and Petekidis (2011)]. In this figure, the yield stress (σ_y) corresponds to the maximum in elastic stress ($G'\gamma$) observed for each concentration, as described by Walls *et al.* (2003). We find σ_y to exhibit a power-law increase with respect to concentration [inset of Fig. 3(b)], i.e., $\sigma_y \sim \varphi^3$. The increase in σ_y possibly arises from the additional links in the network as a result of more NDs being present in the system. Note that a small hump or shoulder is observed in both the elastic stress [Fig. 3(b)] and G'' [Fig. 3(a)] at strains beyond the maxima, which some may attribute to a second yielding [Koumakis and Petekidis (2011)]. However, given the complexity of the system and the subtle observation, we have not probed this further and relegated it for future studies.

Results taken together from Figs. 2 and 3 suggest that G', σ_y, and γ_o all exhibit power-law behavior with respect to ND content. G' and σ_y exhibit positive power-law exponents with that of G' being slightly higher, whereas γ_o reveal a negative index. Buscall and coworkers (1987, 1988) attribute the observed behavior of G' and σ_y of our flocculated network to be comprised a heterogeneous collection of interconnected flocs. Several different particle systems have been suggested to form such colloidal gels including clays, carbon black, and fumed silica [Cassagnua (2008); Kawaguchi *et al.* (2001); and Khan and Zoeller (1993)], in which the materials aggregate via interparticle attractions to form flocs which then interconnect to span the entire sample. Shih and coworkers [1990] have taken this notion of microstructure one step further by incorporating the power-law trend (positive or negative) of the yield strain to classify these materials as weak or strong-linked floc systems. A colloidal gel is considered to be strong-linked if the interactions between the flocs are stronger than within them, thus structural breakdown or yielding occurs via intrafloc breakdown. The yield strain for such systems decreases with increasing particle concentration and exhibits a negative power-law index, i.e., $\gamma_o \sim \varphi^{-p}$. In contrast, a weak-linked system has stronger intrafloc interactions than interfloc interactions, resulting in an increase in yielding strain with particle concentration and a positive power-law index, i.e., $\gamma_o \sim \varphi^p$. Fumed silica systems have been shown to exhibit both weak and strong-linked behavior [Asai *et al.* (2008); Yokoyama *et al.* (2007)], whereas in our case we find our system to be a strong-linked one with γ_o showing a negative power-law index. Note that the trend and not the values of the indices are relevant here, and the different breakdown modes discussed here have been suggested by others as well [Zaccone *et al.* (2009); Del Gado (personal communication)].

B. Microstructure rearrangement

While we have used large amplitude strain measurements to examine the floc structure and yield stress, one of the important issues to determine is to what extent the network reforms following breakdown, and how much this recovery is a function of shear rate, time and degree of breakdown strain [Rueb and Zukoski (1996); Raghavan and Khan (1995)]. We first examined how microstructural breakdown due to steady shear influenced structural recovery and what the role is of shear rate in this regard. Figure 4 shows the frequency spectrum of ND (8 wt. %) samples that have been exposed to steady shear at different shear rates but to the same extent of 500 strain units (50 000% strain). We find that for shear rates studied between 0.1 and 10 s^{-1}, the moduli of the recovered

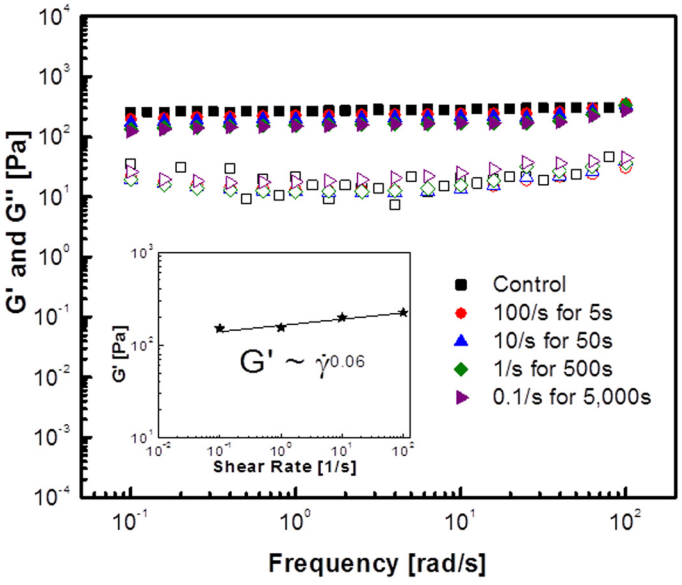

FIG. 4. Dynamic rheology of 8 wt. % NDs in mineral oil (G′ solid symbols, G″ open symbols) after exposure to different steady state strains of 500 by varying shear rate and time. Inset shows the power law dependence of the elastic moduli as a function of shear rate.

sample are similar and essentially equivalent to that of the original sample. In fact, we observe a very weak dependence of shear rate on recovered G′ ($G' \sim \dot{\gamma}^{0.06}$), indicating that possibly extent of deformation and not rate play the dominant role in recovery.

To probe this further, we examined the recovery of NDs in mineral oil by applying a strain outside the linear viscoelastic (LVE) regime. Prior to each experiment, the system was exposed to a frequency sweep ($\omega = 0.1$–100 rad/s, $\gamma = 0.5\%$) to insure reproducibility between samples. Sample breakdown was conducted by exposing it to a breakdown strain of interest for 10 min and measuring G′ as a function of time. Immediately after this, sample recovery was monitored in terms of G′ as a function of time while keeping the strain within the LVE regime (0.5%). The rationale for conducting such experiments stems from a need to understand the role of shear history, both small and large, from scientific and technological viewpoints. The breakdown and recovery of NDs (10 wt. %) in mineral oil are illustrated in Fig. 5(a) as a function of time. Focusing on the first time sweep, or the breakdown step, one can see how a range of strains affect the system's microstructure. Strains below the LVE ($\gamma = 1\%$) do not disrupt the microstructure, as indicated by G′ remaining unchanged. For strains above the LVE ($\gamma = 10$–1000%), G′ decreases from the initial value indicating a disruption in the microstructure that is strain dependent. In addition, most of the breakdown occurs in the first few cycles of applying the sinusoidal strain.

The second time sweep, i.e., the recovery step, shows the system recovers immediately (in less than 30 s) following structural disruption. However, the samples show only a partial recovery, with the G′ of the recovered sample having a lower value than the original sample. In addition, we find the extent of recovery to depend on the breakdown strain applied, which is consistent with other reports [Raghavan and Khan (1995) and Buscall *et al.* (1987)]. In our case we find the recovered G′ to decrease monotonically with increasing breakdown strain to the maximum strain possible with the rheometer (1000%) unlike other aggregated systems such as fumed silica which showed a minimum in recovered G′ followed by full recovery [Raghavan and Khan (1995)]. It should be

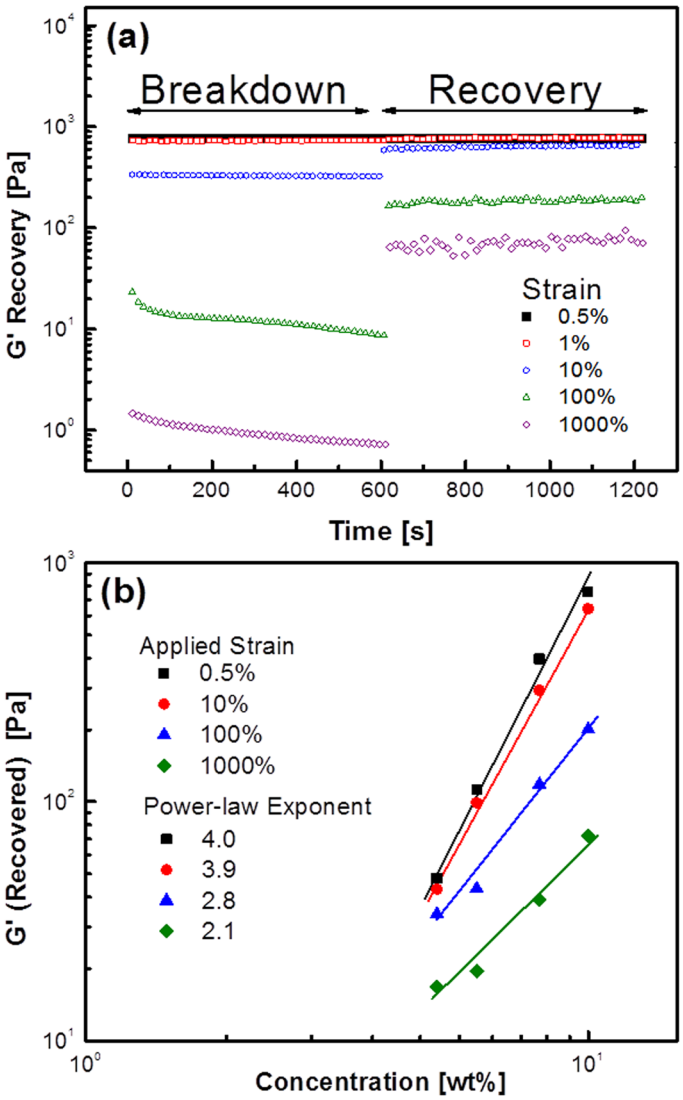

FIG. 5. The structural break down and recovery of 10 wt. % ND in mineral oil (a) at dynamic strains from 0.5–1000% at 1 rad/s as a function of time and (b) at different concentrations to show the power-law dependence of G′ after different strains have been applied.

noted that all recovered samples exhibited gel-like features that remain unchanged after several hours, as was evident from conducting frequency sweep experiments (data not shown) after the system recovery.

The microstructure of these recovered samples were examined by plotting the recovered $G'(\omega = 1\,\text{rad/s})$ as a function of ND concentration for each breakdown strain applied [Fig. 5(b)]. We find that all strained material systems show a power-law behavior, i.e., $G' \sim \varphi^n$, where n varies with the extent of breakdown strain. The fact that samples show a scaling relationship suggests that the mechanism of structural breakdown and reformation is independent of concentration; however, different microstructures are formed depending on breakdown strain as the power-law exponents are functions of strain. Samples in which the applied breakdown strains were near the LVE (0.5–10%) have a

similar power-law exponents near 4, which is similar what is reported in colloidal literature [Khan and Zoeller (1993); Rueb and Zukoski (1996); Wu *et al.* (2012)]. For larger strains, the value of the power-law exponents for the recovered material decrease with increasing strain, indicating a weaker microstructure. Similar exponent decreases for sheared colloidal gels have been previously reported [Paquien *et al.* (2005)].

We attempt to explain the structural breakdown and reformation of the NDs pictorially using the idealized schematics in Fig. 6. We speculate that exposure of NDs to oscillatory strains leads to breakage of intrafloc bonds (Fig. 6, top). Cessation of shear allows the microstructure to rearrange into larger flocs with fewer linkages between them. This could explain the reduction in modulus and in power-law exponent for recovered NDs. In the case of steady shear, the significantly larger strain essentially breaks the microstructure down completely (Fig. 6, bottom), allowing it to reform to its original configuration. The microstructure breakdown analogy is consistent with our findings of a strong-linked flocculated system, and has also been reported for other attractive systems [Raghavan and Khan (1995); Paquien *et al.* (2005); Zaccone *et al.* (2009); Del Gado (personal communication)].

C. ND interactions

Our rheology data, in combination with particle size measurements indicate that we have tightly bound aggregates that group together to form flocs that span the entire sample. Studies suggest that NDs flocculation is due to a combination of van der Waals (VDW) attraction and hydrogen bonding between the oxygen rich groups attached to the ND core [Xu and Zhao (2012); Mochalin *et al.* (2011); Krueger (2008)]. The presence and impact of these interactions in the ND/mineral oil system therefore need to be considered. We start by examining the presence of VDW attraction within the mineral oil system by comparing the Hamaker constants [Israelachvili (2001); Vincent (1973); Vold (1961)] of the ND particle (A_p) and mineral oil, the solvent media (A_m). We find the Hamaker constant for mineral oil to be 6.29×10^{-20} J whereas that of the NDs is 29.6×10^{-20} J [Israelachvili (2001); Vincent (1973); Lui *et al.* (2012)]. Given the difference in Hamaker constant between ND and mineral oil, and the fact that the net VDW forces are related through the difference in Hamaker constants ($V_{vdW} \sim (\sqrt{A_m} - \sqrt{A_p})^2$), it is evident that attractive VDW forces are prevalent in our system.

Hydrogen-bonding interactions are also known to affect gel formation, depending on the nature of the particles and solvents used. Raghavan *et al.* (2000a) were able to relate

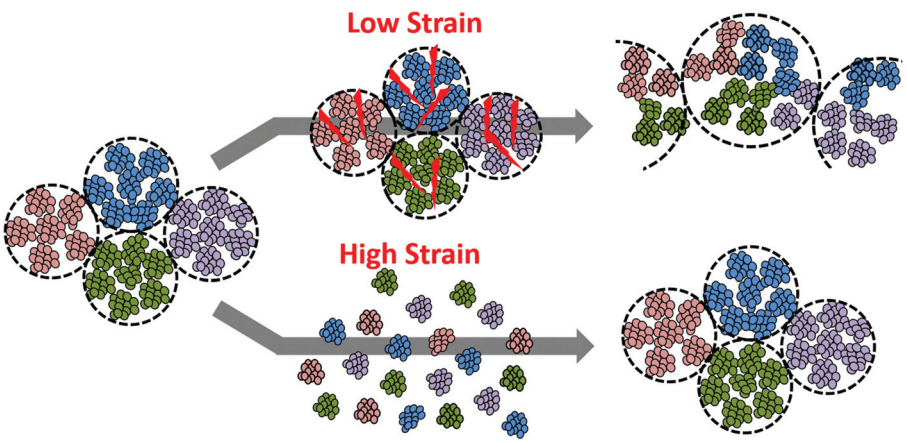

FIG. 6. Schematic representation of the floc microstructure in the ND/mineral oil system during and after oscillatory shear. The red lines in the top intermediate schematic imply a breakdown of intrafloc linkages.

the formation of silica gels to the hydrogen-bonding strength of the solvent. If the hydrogen bonds of the particle interact with strong hydrogen-bonding sites on the solvent molecule, then a stable solution is possible due to hydration forces. If the solvent has a low hydrogen-bonding ability, like mineral oil (dielectric constant of 2.1), then the particles interact directly with each other instead of the hydrophobic solvent and a colloidal gel is possible. This is the case of NDs dispersed in mineral oil with the NDs hydrogen bonding with each other and not mineral oil. We believe that this interaction, in combination with the VDW attractions leads to the formation of ND flocs that span the sample and create a colloidal gel. Huang *et al*. (2008), Mochalin *et al*. (2011), and Krueger (2008) have proposed similar mechanisms for ND-ND agglomeration, and Raghavan *et al*. (2000b) have proposed comparable mechanisms for the formation of fumed silica colloidal gels.

To further probe the importance of hydrogen-bonding in the case of NDs, we have functionalized NDs with a methacrylate moiety (3-MPTS) and studied the resulting particles in mineral oil. We postulated that the methacrylate moieties will introduce steric hindrance and thus interfere with the hydrogen-bonding ability of the particles. ND functionalization with 3-MPTS is expected to proceed in three stages (Fig. 7). Each stage of the reaction was verified via FTIR spectroscopy [Fig. 8(a)] and resulted in a color change. The raw NDs show a predominant hydroxyl peak at 3417 cm^{-1}, with additional peaks around 2900, 1790, 1630, and 1385 cm^{-1} that Morimune *et al*. (2011) report to be C-H stretching, carbonyl, C=C stretching, and C-H deformation, respectively. Oxidation of NDs results in increases of the carbonyl groups (i.e., carboxylic acid, 1784 cm^{-1}) and decreases in C-H stretching (2900 cm^{-1}) and deformation (1385 cm^{-1}), as expected

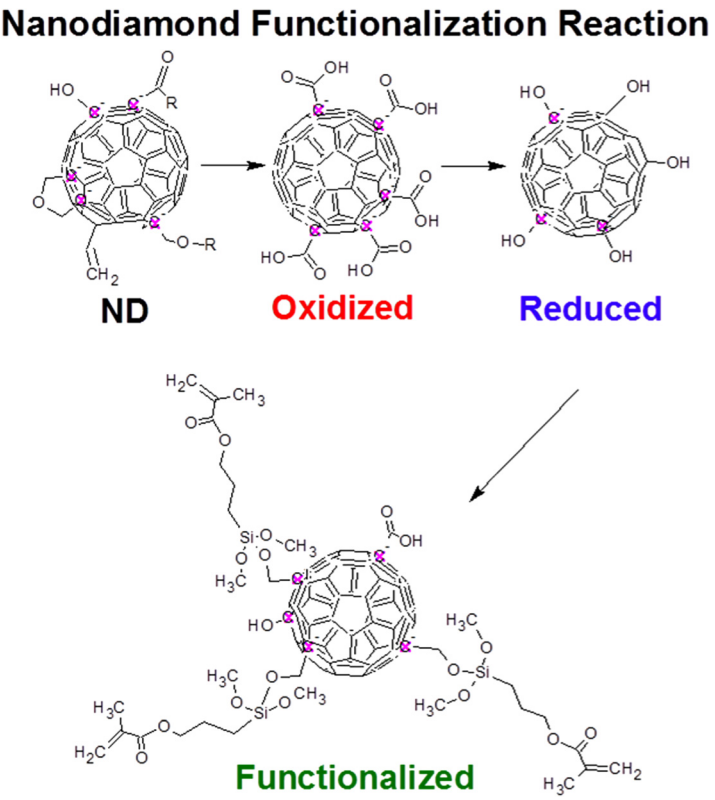

FIG. 7. Schematic representation of the ND structural changes after oxidation, reduction and 3-MPTS functionalization.

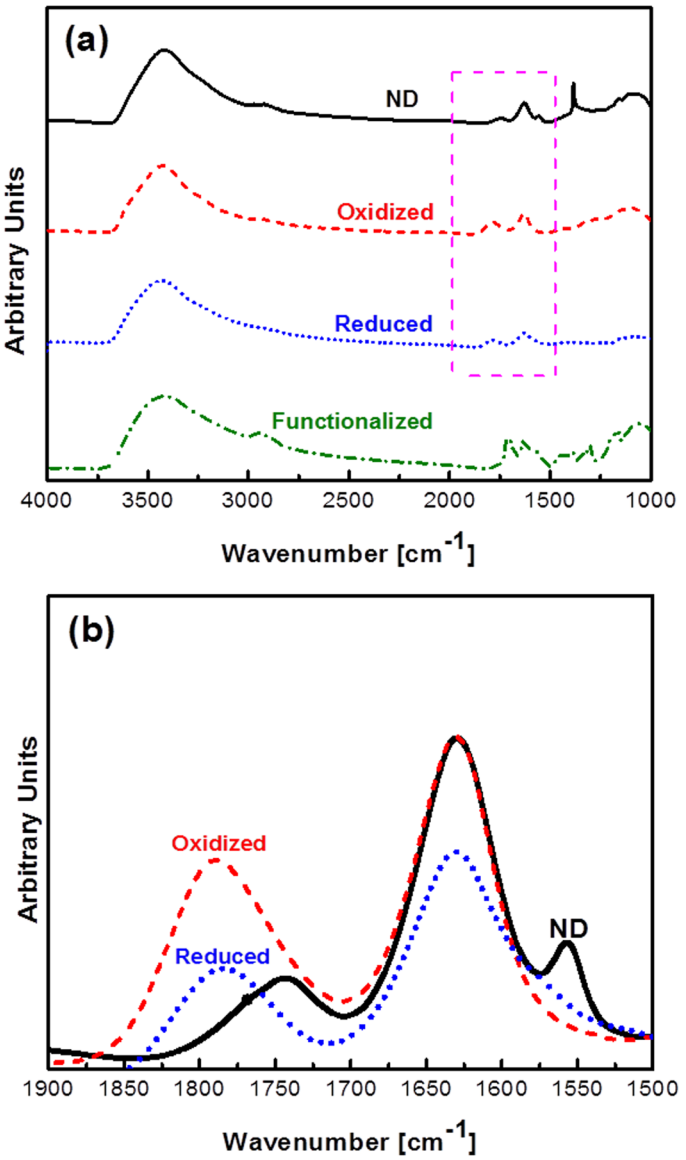

FIG. 8. FTIR spectra of (a) NDs (solid), oxidized ND (dash), reduced ND (dot), and functionalized (dotted/dashed) NDs, and (b) zoomed in FTIR spectra to show C=C and carbonyl peaks.

because oxidation removes carbon impurities by converting surface organic groups to carbonyls [Fig. 8(b)]. The reduction step then further reduces the carbonyl groups to hydroxyl groups, as indicated by a peak decrease at 1784 cm^{-1}. This addition and then the removal of carbonyl groups during oxidation and reduction have been previously reported during the oxidation and reduction of carbon nanotubes [Irani *et al.* (2013)]. Finally, the reaction of 3-MPTS functional groups results in peaks at 1063, 1169, 1300, 1325, and 1630 cm^{-1} due to the addition of Si-O-C bonding, Si-OH propyl chains, and increased C=C stretching, respectively. Similar spectrum changes have been reported by Bag *et al.* (2004) during the addition of 3-MPTS to carbon nanotubes.

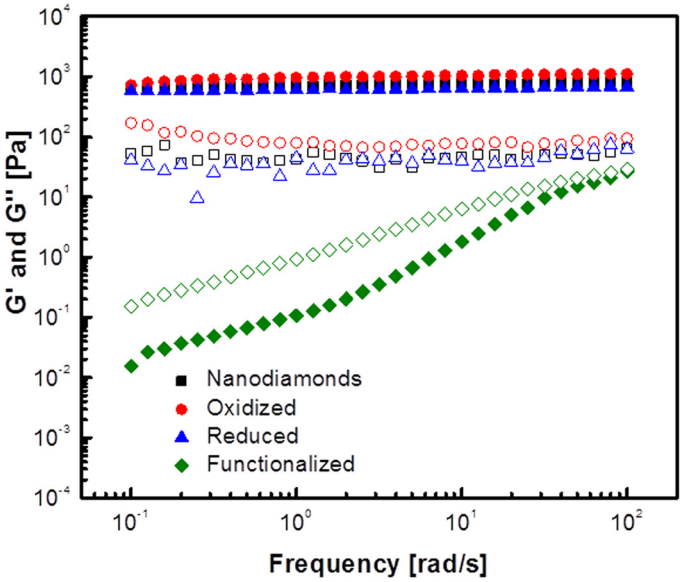

FIG. 9. Dynamic moduli of 10 wt. % untreated (square), oxidized (circle), reduced (triangle), and functionalized NDs in mineral oil as a function of frequency. G′ corresponds to the solid symbols whereas G″ to the open symbols.

Visual and rheological experiments were conducted after each reaction stage in order to examine whether colloidal gel formation was affected. Oxidized and reduced NDs in mineral oil behave similar to the untreated NDs, i.e., gave rise to gel-like samples, as seen by the frequency spectra in Fig. 9. Similar moduli are observed because the hydrogen-bonding groups and VDW interaction are minimally affected by the oxidation and reduction steps. However, methacrylate-functionalized NDs behave differently; the frequency spectra show a viscoelastic response with both moduli varying with frequency. However, no terminal regime is observed indicating that VDW interactions still exist possibly leading to weak flocculation. The dispersion remains stable and does not exhibit precipitation or gel formation for extended periods leading us to postulate that functionalizing the ND surface with methacrylate groups leads to a decrease in the hydrogen bonding needed for colloidal gel formation. In order for hydrogen bonding to occur both a hydrogen bond acceptor (an electronegative atom like oxygen) and donor (hydrogen attached to an electronegative atom) are needed [Perrin and Nielson (1997)]. The untreated ND surface is populated with both hydrogen bond acceptors and donors; however, the methacrylate-functionalized group only has hydrogen bond acceptors. In addition to the lack of hydrogen bond donors, the methacrylate-functionalized group is relatively bulky, approximately 15 Å in length. This bulkiness acts as a barrier that shields unreacted hydrogen bond donors left over from the original ND surface, making any potential hydrogen bonding difficult. The introduction of steric hindrances and thereby reducing hydrogen-bonding donor sites thus provide a facile approach to control and tune ND gelation.

IV. CONCLUSIONS

The viscoelastic properties of NDs in mineral oil were studied using dynamic and steady shear rheology. The particles were observed to form colloidal gels that exhibited

elastic rheological behavior. The elastic modulus (G′), yield stress (σ_y), and yield strain (γ_o) of these gels all scaled with ND concentration, with G′ and σ_y exhibiting positive power-law exponents and γ_o showing a negative one. Such behavior is consistent with a gel network composed of strong-linked flocs. Large oscillatory strains were applied to the samples to investigate the microstructure breakdown and recovery. The results indicate that formation and rearrangement of the ND microstructures are concentration and strain dependent with the colloidal gel formation attributed to a combination of VDW and hydrogen-bonding interactions. Surface modifications with reduced hydrogen bonding were found to hinder gel formation and resulted in a stable dispersion, thus providing a route to modulate gel formation.

References

Asai, H., A. Masuda, and M. Kawaguchi, "Rheological properties of colloidal gels formed from fumed silica suspensions in the presence of cationic surfactants," J. Colloid Interface Sci. **328**, 180–185 (2008).

Bag, D. S., R. Dubey, N. Zhang, J. Xie, V. K. Varadan, D. Lal, and G. N. Mathur, "Chemical functionalization of carbon nanotubes with 3-methacryloxypropyltrimethoxysilane (3-MPTS)," Smart Mater. Struct. **13**, 1263–1267 (2004).

Buscall, R., I. J. Mcgowan, P. D. A. Mills, R. F. Stewart, D. Sutton, L. R. White, and G. E. Yates, "The rheology of strongly-flocculated suspensions," J. Non-Newtonian Fluid **24**, 183–202 (1987).

Buscall, R., P. D. A. Mills, J. W. Goodwin, and D. W. Lawson, "Scaling behavior of aggregated networks formed from colloidal particles," J. Chem. Soc. Faraday Trans. I **84**, 4249–4260 (1988).

Cassagnau, P., "Melt rheology of organoclay and fumed silica nanocomposites," Polymer **49**, 2183–2196 (2008).

Del Gado, E., personal communications, Attractive Colloids & Gels Meeting, Hellenic Society of Rheology (HSR14), Crete, July 2014.

Goertzen, S. L., K. D. Theriault, A. M. Oickle, A. C. Tarasuk, and H. A. Andreas, "Standardization of the Boehm titration. Part 1. CO_2 expulsion and endpoint determination," Carbon **48**, 1252–1261 (2010).

Huang, H., L. Dai, D. H. Wang, L. Tan, and E. Osawa, "Large-scale self-assembly of dispersed nanodiamonds," J. Mater. Chem. **18**, 1347–1352 (2008).

Hui, Y. Y., C. Cheng, and H. Chang, "Nanodiamonds for optical bioimaging," J. Phys. D: Appl. Phys. **43**, 374021 (2010).

Irani, F., A. Jannesari, and S. Bastani, "Effect of fluorination of multiwalled carbon nanotubes (MWCNTs) on the surface properties of fouling-release silicone/MWCNTs coatings," Prog. Org. Coat. **76**, 375–383 (2013).

Israelachvili, J., *Intermolecular and Surface Forces*, 2nd ed. (Elsevier, Waltham, MA, 2001), pp. 176–185.

Kawaguchi, M., M. Okuno, and T. Kato, "Rheological properties of carbon black suspensions in a silicone oil," Langmuir **17**, 6041–6044 (2001).

Khan, S. A., C. A. Schnepper, and R. C. Armstrong, "Foam rheology: III. Measurement of shear flow properties," J. Rheol. **32**, 69–92 (1988).

Khan, S. A., and N. J. Zoeller, "Dynamic rheology behavior of flocculated fumed silica suspensions," J. Rheol. **37**, 1225–1235 (1993).

Kotov, N. A., "Inorganic nanoparticles as protein mimics," Science **330**, 188–189 (2010).

Koumakis, N., and G. Petekidis, "Two-step yielding in attractive colloids: Transition from gels to attractive glasses," Soft Matter **7**, 2456–2470 (2011).

Krueger, A., "New carbon materials: Biological applications of functionalized nanodiamond materials," Chem. Eur. J. **14**, 1382–1390 (2008).

Krueger, A., "Beyond the shine: Recent progress in applications of nanodiamond," J. Mater. Chem. **21**, 12571–12578 (2011).

Krueger, A., F. Kataoka, M. Ozawa, T. Fujino, Y. Suzuki, A. E. Aleksenskii, A. Y. Vul, and E. Osawa, "Unusually tight aggregation in detonation nanodiamond: Identification and disintegration," Carbon **43**, 1722–1730 (2005).

Liu, X., T. Yu, Q. Wei, Z. Yu, and X. Xu, "Enhanced diamond nucleation on copper substrates by employing an electrostatic self-assembly seeding process with modified nanodiamond particles," Colloids Surf., A **412**, 82–89 (2012).

Liu, Y., Z. Gu, J. L. Margrave, and V. N. Khabashesku, "Functionalization of nanoscale diamond powder: Fluoro-, alkyl-, amino-, and amino acid-nanodiamond derivatives," Chem. Matter. **16**, 3924–3930 (2004).

Marchesan, S., M. Melchionna, and M. Prato, "Carbon nanostructures for nanomedicine: Opportunities and challenges," Fullerenes Nanotubes Carbon Nanostruct. **22**, 190–195 (2014).

Mochalin, V. N., I. Neitzel, B. J. M. Etzold, A. Peterson, G. Palmese, and Y. Gogotsi, "Covalent incorporation of aminated nanodiamond into an epoxy polymer network," ACS Nano **5**, 7494–7502 (2011).

Mochalin, V. N., O. Shenderova, D. Ho, and Y. Gogotsi, "The properties and applications of nanodiamonds," Nat. Nanotechnol. **7**, 11–23 (2012).

Moller, P. C. F., J. Mewis, and D. Bonn, "Yield stress and thixotropy: On the difficulty of measuring yield stress in practice," Soft Matter **2**(4), 274–283 (2006).

Morimune, S., M. Kotera, T. Nishino, K. Goto, and K. Hata, "Poly (vinyl alcohol) nanocomposites with nanodiamond," Macromolecules **44**, 4415–4421 (2011).

Ozawa, M., M. Inakuma, M. Takahashi, F. Kataoka, A. Krueger, and E. Osawa, "Preparation and behavior of brownish, clear nanodiamond colloids," Adv. Mater. **19**, 1201–1206 (2007).

Paquien, J. N., J. Galy, J. F. Gerard, and A. Pouchelon, "Rheological studies of fumed silica-polydimethylsiloxane suspensions," Colloids Surf., A **260**, 165–172 (2005).

Perrin, L. C., and J. B. Nielson, "Strong hydrogen bonds in chemistry and biology," Ann. Rev. Phys. Chem. **48**, 511–544 (1997).

Raghavan, S. R., J. Hou, G. L. Baker, and S. A. Khan, "Colloidal interactions between particles with tethered nonpolar chains dispersed in polar media: Direct correlation between dynamic rheology and interaction parameters," Langmuir **16**, 1066–1077 (2000b).

Raghavan, S. R., J. H. J. Walls, and S. A. Khan, "Rheology of silica dispersions in organic liquids: New evidence of salvation forces dictated by hydrogen bonding," Langmuir **16**, 7920–7930 (2000a).

Raghavan, S. R., and S. A. Khan, "Shear-induced microstructural changes in flocculated suspensions of fumed silica," J. Rheol. **39**, 1311–1325 (1995).

Rueb, C. J., and C. F. Zukoski, "Viscoelastic properties of colloidal gels," J. Rheol. **41**, 197–218 (1996).

Schrand, A. M., S. A. C. Hens, and O. A. Shenderova, "Nanodiamond particles: Properties and perspectives for bioapplications," Crit. Rev. Solid State Mater. Sci. **34**, 18–74 (2009).

Shay, J. S., S. R. Raghavan, and S. A. Khan, "Thermoreversible gelation of aqueous dispersions of colloidal particles bearing grafted poly(ethylene oxide) chains," J. Rheol. **45**, 913–928 (2001).

Shih, W.-H., W. Y. Shih, and I. A. Aksay, "Elastic and yield behavior of strongly flocculated colloids," J. Am. Ceram. Soc. **82**, 616–624 (1999).

Shih, W.-H., W. Y. Shih, S. Kim, J. Liu, and I. A. Aksay, "Scaling behavior of the elastic properties of colloidal gels," Phys. Rev. A **42**, 4772–4779 (1990).

Thalhammer, A., R. J. Edgington, L. A. Cingolani, R. Schoepfer, and R. B. Jackman, "The use of nanodiamond monolayer coatings to promote the formation of functional neuronal networks," Biomaterials **31**, 2097–2104 (2010).

Vast, L., Z. Mekhalif, A. Fonseca, J. B. Nagy, and J. Delhalle, "Preparation and electrical characterization of a silicone elastomer composite charged with multi-wall carbon nanotubes functionalized with 7-octenyltrichlrosilane," Compos. Sci. Technol. **67**, 880–889 (2007).

Vincent, B., "The van der Waals attraction between colloid particles having adsorbed layers. II. Calculation of interaction curves," J. Colloid Interface Sci. **42**, 270–285 (1973).

Vold, M., "The effect of adsorption on the van der Waals interaction of spherical colloidal particles," J. Colloid Interface Sci. **16**, 1–12 (1961).

Vreeker, R., L. L. Hockstra, D. C. den Boer, and W. G. M. Agterof, "The fractal nature of fat crystal networks," Colloids Surf. **65**, 185–189 (1992a).

Vreeker, R., L. L. Hockstra, D. C. den Boer, and W. G. M. Agterof, "Fractal aggregation of whey proteins," Food Hydrocolloids **6**, 423–435 (1992b).

Walls, H. J., S. B. Caines, A. M. Sanchez, and S. A. Khan, "Yield stress and wall slip phenomena in colloidal silica gels," J. Rheol. **47**, 847–868 (2003).

Wu, X., Y. Wang, W. Yang, B. Xie, M. Yang, and W. Dan, "A rheological study on temperature dependent microstructural changes of fumed silica gels in dodecane," Soft Matter **8**, 10457–10463 (2012).

Xu, Q., and X. Zhao, "Electrostatic interactions versus van der Waals interactions in the self-assembly of dispersed nanodiamonds," J. Mater. Chem. **22**, 16416–16421 (2012).

Yang, M. C., L. E. Scriven, and C. W. Macosko, "Some rheological measurements on magnetic iron oxide suspensions in silicone oil," J. Rheol. **30**, 1015–1029 (1986).

Yokoyama, K., Y. Koike, A. Masuda, and M. Kawaguchi, "Rheological properties of fumed silica suspensions in the presence of potassium chloride," Jpn. J. Appl. Phys., Part 1 **46**, 328–332 (2007).

Zaccone, A., H. Wu, and E. Del Gado, "Elasticity of arrested short-range attractive colloids: Homogeneous and heterogeneous glasses," Phys. Rev. Lett. **103**, 208301 (2009).

Zhang, B., X. Zheng, and H. Li, "Application of carbon-based nanomaterials in sample preparation: A review," Anal. Chim. Acta **784**, 1–17 (2013).